

Draft of the article published by the Journal of Vibration and Control 22 (2016)
DOI: 10.1177/1077546314547728.

A methodology for damping measurement of engineering materials: application to a structure under bending and torsion loading.

Armando Pérez-Peña, Andrés A García-Granada*, Joaquín Menacho, José J Molins and Guillermo Reyes

IQS School of Engineering, Universitat Ramon Llull, Barcelona, Spain

Introduction

An engineer does not need to consider damping for most of static (long term load) calculations, as loads and displacements are considered to be constant. Nevertheless, for a dynamic calculation a more realistic frequency response is needed. When resonance and signal amplification have to be taken into account, accurate damping ratio values are of great concern. In these cases, most of the energy is considered to be absorbed as plastic deformation and damping cannot be ignored. Usually damping is introduced with unrealistically high values (above 10%) in order to obtain a stable solution using explicit integration.

Computer simulation is widely used in engineering calculation to obtain reasonable results at a low cost and far quicker in comparison to experimental approaches. Properties such as Young's modulus, density, thermal expansion coefficient or yield stress are well covered in most material databases for simulation.

Although the damping ratio of common materials is relevant for engineering applications, there is a lack of information about it in many computer assisted applications. As an example, the materials databases for SolidWorks™ 2011 and Ansys Workbench™ 13 were examined and the materials damping ratio was not provided in either of these.

In order to measure the damping ratio of a material, the vibrating beam method as specified in ASTM E756-05 (Xu and Nashif, 1996, Erdoğan and Bayraktar, 2003,

* *Corresponding author:* Andrés A. García-Granada, IQS School of Engineering, Via Augusta 390, 08017 Barcelona (Spain), Email: andres.garcia@iqs.edu

Wojtowicki *et al.*, 2004, Crespo *et al.*, 2010) is commonly used. The ASTM E756-05 standard recommends the half-power bandwidth (HPB) method reported by Wei and Kukureka (2000) and Orban (2011) for evaluating the modal loss factor. Although this method provides an accurate estimation of the modal loss factor for lightly damped specimens, the error increases exponentially with the modal loss factor (Martínez-Aguirre and Elejaberrieta, 2010). Foss (2007) used an alternative method to measure damping at several temperatures. Malogi, Gupta and Kathawate (2009) developed the center impedance method as an alternative option. Wei and Kukureka (2000) used a method based on the power band width together with free-decay in order to examine the damping ratio for composites. When the material to be analyzed is a damper, its first resonance natural frequency is commonly measured in order to obtain its damping ratio using a band width method (Cai and Sun, 2010).

Most of the documented work on damping measurement is focused on composites (Brodth and Lakes, 1995; Wei and Kukureka, 2000; Hammami *et al.*, 2005; Foss, 2007; Martínez-Aguirre and Elejaberrieta, 2010) and dampers which have a high damping ratio (Cai and Sun, 2010; Foss, 2007; Martínez-Aguirre and Elejaberrieta, 2010). There are less studies focusing on the damping of a real structure of several assembled parts (Chowdhuri and Dasgupta, 2003; Orban, 2011). Regarding the application of the damping ratio on simulation, with the Finite Element Method (FEM), Jáuregui *et al.* (2005) compared their measurements to simulations on torsional vibrations of elastomeric components. Ilg *et al.* (2012) used a reverse damping ratio approach to characterize a silicone rubber. Finally Chowdhuri and Dasgupta (2003) analyzed the issue of introducing Rayleigh damping parameters for simulations of civil engineering structures.

The development time for new products in the industry is shrinking. This forces engineers to quickly evaluate the mechanical performance of the product, which prevents carrying out damping tests of materials if they are too time consuming or require expensive equipment, or both. Thus, the main objective of this study is to develop an accurate, cheap and quick method to measure damping of materials and structures applicable to Finite Element Method (FEM) simulations. This it is achieved by the experimental work, simulations and correlations laid out in this paper.

Several experiments to measure damping for different specimens are described. Measured damping results were introduced in simulations to reproduce the experiment and check the methodology. Measurements for several parameter modifications such as frequency, sampling rate, number of periods to read, etc. are also described. Finally this method is applied to a structure that works under resonance for torsion and bending in order to check

the usefulness of the method for real structures. Literature was reviewed to focus on the way of measuring damping and considering it in simulations.

Theoretical background

Theoretical resonance frequency of a cantilever beam.

The explanation is based on a planar model of a cantilever beam where space is described with an (x, y) reference coordinate system. The beam has a flexural deformation with displacement measured along the y -axis satisfying the following equation:

$$\frac{\partial^4 y}{\partial x^4} + \frac{\rho A}{EI} \cdot \frac{\partial^2 y}{\partial t^2} = 0 \quad (1)$$

where ρ is the density of the beam material, A is the cross section area of the beam, E is Young's modulus, and I is the cross section inertia of the beam. The equation can be solved as follows:

$$y(x, t) = \left[A \cos \sqrt{\frac{\omega_n}{\sigma}} x + B \sin \sqrt{\frac{\omega_n}{\sigma}} x + C \cosh \sqrt{\frac{\omega_n}{\sigma}} x + D \sinh \sqrt{\frac{\omega_n}{\sigma}} x \right] \cdot \sin(\omega_n t + \phi) \quad (2)$$

with:

$$\sigma^2 = \frac{EI}{\rho A} \quad (3)$$

where ω_n is the n -th natural angular frequency of vibration.

For a cantilever beam of length L , with no displacement and no rotation at $x = 0$, and zero bending moment and shear at free end $x = L$, the solution is simplified using the following boundary conditions:

$$\begin{aligned} y(0, t) = 0 & \quad \frac{\partial y}{\partial x}(0, t) = 0 \\ \frac{\partial^2 y}{\partial x^2}(L, t) = 0 & \quad \frac{\partial^3 y}{\partial x^3}(L, t) = 0 \end{aligned} \quad (4)$$

Applying such boundary conditions to equation (2) natural frequencies are obtained by solving the following equation:

$$\cos \sqrt{\frac{\omega_n}{\sigma}} L \cdot \cosh \sqrt{\frac{\omega_n}{\sigma}} L = -1 \quad (5)$$

The roots of such an equation provide the following natural frequencies:

$$\begin{aligned} \omega_1 &= 0,597^2 \sigma \frac{\pi^2}{L^2} \text{ [rad/s]} & \rightarrow & f_1 = \frac{1}{2\pi} \sqrt{\frac{3EI}{0,2424m_b L^3}} \text{ [Hz]} \\ \omega_2 &= 1,49^2 \sigma \frac{\pi^2}{L^2} \text{ [rad/s]} & \rightarrow & f_2 = \frac{(4-1)^2}{2\pi} \sqrt{\frac{3EI}{0,5061m_b L^3}} \text{ [Hz]} \\ \omega_3 &= 2,5^2 \sigma \frac{\pi^2}{L^2} \text{ [rad/s]} & \rightarrow & f_3 = \frac{(6-1)^2}{2\pi} \sqrt{\frac{3EI}{0,4928m_b L^3}} \text{ [Hz]} \\ \omega_n &\approx (2n-1)^2 \frac{\pi^2}{4} \cdot \frac{\sigma}{L^2} \text{ [rad/s]} & \rightarrow & f_4 = \frac{(2n-1)^2}{2\pi} \sqrt{\frac{3EI}{0,4928m_b L^3}} \text{ [Hz]} \quad , n > 3 \end{aligned} \quad (6)$$

It is possible to apply these formulae to the case of a rectangular beam cross section as follows:

$$\begin{aligned} f_1 &= \frac{1}{2\pi} \sqrt{\frac{3EI}{0,2424m_b L^3}} = \frac{1}{2\pi} \sqrt{\frac{Eh^2}{0,9698\rho L^4}} \text{ [Hz]} \\ f_2 &= \frac{(4-1)^2}{2\pi} \sqrt{\frac{3EI}{0,5061m_b L^3}} = \frac{(4-1)^2}{2\pi} \sqrt{\frac{3Eh^2}{2,025\rho L^4}} \text{ [Hz]} \\ f_3 &= \frac{(6-1)^2}{2\pi} \sqrt{\frac{3EI}{0,4928m_b L^3}} = \frac{(6-1)^2}{2\pi} \sqrt{\frac{3Eh^2}{1,971\rho L^4}} \text{ [Hz]} \\ f_n &\approx \frac{(2n-1)^2}{2\pi} \sqrt{\frac{3EI}{0,4928m_b L^3}} = \frac{(2n-1)^2}{2\pi} \sqrt{\frac{3Eh^2}{1,971\rho L^4}} \text{ [Hz]} \quad , n > 3 \end{aligned} \quad (7)$$

where m_b is the mass of the beam, L the length, h is the height and b the width of the rectangular cross section.

Resonance frequency of a cantilever beam with a mass attached to the free end.

The same bending relation defined by equation (1) is applicable to this new situation but with a slight change in boundary conditions. A mass has been attached to the free end thereby introducing acceleration which interacts as an inertial force. The new boundary conditions are:

$$\begin{aligned} y(0,t) &= 0 & \frac{\partial y}{\partial x}(0,t) &= 0 \\ \frac{\partial^2 y}{\partial x^2}(L,t) &= 0 & EI \frac{\partial^3 y}{\partial x^3}(L,t) &= m \frac{\partial^2 y}{\partial t^2}(L,t) \end{aligned} \quad (8)$$

These boundary conditions assume that the mass is placed at one point right at the tip of the beam and therefore there is no bending moment at the free end with the added mass but just shear. Solving equation (2) with these new boundary conditions, natural frequencies might be found as roots of the following expression:

$$1 + \cos \sqrt{\frac{\omega_n}{\sigma}} L \cdot \cosh \sqrt{\frac{\omega_n}{\sigma}} L = \frac{m}{m_b} \sqrt{\frac{\omega_n}{\sigma}} L \cdot \left[\sin \sqrt{\frac{\omega_n}{\sigma}} L \cdot \cosh \sqrt{\frac{\omega_n}{\sigma}} L - \cos \sqrt{\frac{\omega_n}{\sigma}} L \cdot \sinh \sqrt{\frac{\omega_n}{\sigma}} L \right] \quad (9)$$

It is observed that equation (9) is identical to equation (5) when $m=0$. By using a notation to the unknown $\gamma = L\sqrt{\omega_n/\sigma}$ and by means of numerical methods the first natural frequency is solved as a function of the ratio of mass tip m to the mass of the beam m_b . These values are plotted in Table 1.

Table 1: values of frequency parameter γ [rad] as function of mass ratio [-].	
m/m_b	γ
100	0.4160
50	0.4943
20	0.6205
10	0.7357
5	0.8610
3	0.9812
2	1.0762
1	1.2479
0.5	1.4110
0.2	1.6164
0.1	1.7227
0.05	1.7912
0.02	1.8393
0.01	1.8568

With these values the first angular frequency is calculated as follows:

$$\omega_1 = \frac{\gamma^2}{L^2} \sigma \quad [\text{rad/s}] \rightarrow f_1 = \frac{1}{2\pi} \sqrt{\frac{\gamma^4 EI}{m_b L^3}} \quad [\text{Hz}] \quad (10)$$

By means of the least squares method, a good approximation to the value of γ in the whole range of table 1 is obtained as:

$$\gamma^4 \approx \frac{1}{0,3332 \cdot \frac{m}{m_b} + 0,0803} \quad (11)$$

$$f_1 \approx \frac{1}{2\pi} \sqrt{\frac{3EI}{L^3(m + 0,2409 \cdot m_b)}} \quad [\text{Hz}] \quad (12)$$

In this case the factor applied to the mass of the beam is 0.2409 which differs from the 0.2424 shown in equation (7) for $m=0$.

Equations of linear model with damping.

When conditions lead to a small deformation, the behavior of the first mode of vibration of a cantilever beam can be approximated to the behavior of a one degree of freedom mass-spring-damper system. (Fig. 1).

Vibration of such a linear system is described by the well-known equation:

$$\ddot{x} + 2\xi\omega_1\dot{x} + \omega_1^2 x = 0 \quad (13)$$

Where the resonance angular frequency is $\omega_1 = \sqrt{k/m}$ and the damping ratio

$$\xi = \frac{c}{2\sqrt{km}} = \frac{c}{2m\omega_1} \quad (14)$$

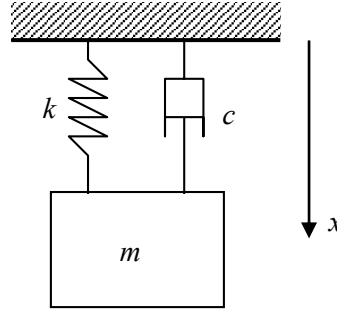


Fig. 1: Linear model: m = mass, c = damping coefficient, k = elastic stiffness

where k is the stiffness, c is the damping coefficient and m is the mass. The general solution to this equation is obtained as follows:

$$x(t) = A \cdot e^{-\xi\omega_1 t} \cdot \cos(\omega_1 \sqrt{1-\xi^2} \cdot t + \varphi) \quad (15)$$

If the tip of the cantilever beam is driven to an initial displacement and then left free to oscillate, the vibration is analytically obtained for the following initial conditions: $x(0) = x_0$; $x'(0) = 0$. In this case the value of the vibration amplitude and phase are as follows:

$$A = \frac{x_0}{\sqrt{1-\xi^2}} \quad ; \quad \varphi = \arctan \frac{-\xi}{\sqrt{1-\xi^2}} \quad (16)$$

The method to measure the damping coefficient described in this work consists of the determination of parameters ξ and ω_1 in order to adjust equation (15) to the experimental data measured of a vibrating cantilever beam.

Fitting of experimental data to vibration equations.

In order to determine the natural frequency and damping ratio, a test specimen, fixed at one end (Figure 2), is moved away from the static equilibrium position. The displacement of its free end is measured using a laser transducer. The parameters of the formula (15) are adjusted to the data collected using the least squares method, with a Nelder-Mead Simplex algorithm. The optimization parameters are A , φ , ω_1 and ξ .

Finite Elements calculations with damping.

In ANSYS™ there are several ways to introduce the damping factor, each of them being suitable for a particular case. In this case -a transient dynamic analysis- the way to enter the damping factor is by Rayleigh's equivalent damping. The free vibration equation for a structure is formulated as:

$$(m)\ddot{x} + (c)\dot{x} + (k)x = 0 \quad (17)$$

where x is a vector representing the displacement of every element of the structure (or every element, in FEM calculations), and (m) , (c) and (k) are the mass, damping and stiffness matrices. Rayleigh's theory assumes that the damping matrix (c) is a function of mass and stiffness matrices that can be linearized with α and β as constants that multiply the matrices of mass (m) and stiffness (k) :

$$(c) = \alpha(m) + \beta(k) \quad (18)$$

As a consequence of the mathematical theory of matrices, the same orthogonal transformation that allows to diagonalize (m) and (k) allows to diagonalize (c) . This allows for the equivalent expression:

$$(M)\ddot{\eta} + (C)\dot{\eta} + (K)\eta = 0 \quad (19)$$

where (M) , (C) and (K) are the diagonalized matrices, for a set of coordinates η (modal coordinates). System (19) is a set of uncoupled equations. For each mode of vibration, there is an equation:

$$M_{ii} \cdot \ddot{\eta}_i + C_{ii} \cdot \dot{\eta}_i + K_{ii} \cdot \eta_i = 0 \quad (20)$$

that can also be written as (13):

$$\ddot{\eta}_i + 2\xi_i \omega_i \cdot \dot{\eta}_i + \omega_i \cdot \eta_i = 0 \quad (21)$$

where ω_i and ξ_i are the resonance angular frequency and damping ratio of the i -th mode, respectively.

The damping ratio for each mode of vibration, from (20), satisfies the following equation:

$$2\xi_i\omega_i = \frac{C_{ii}}{M_{ii}} \Rightarrow \xi_i = \frac{\alpha M_{ii} + \beta K_{ii}}{2\sqrt{K_{ii}M_{ii}}} = \frac{\alpha}{2\omega_i} + \frac{\beta\omega_i}{2} \quad (22)$$

More details about Rayleigh's model of damping can be found in Rao (1986), Newland (1989), Gatti and Ferrari (1999), Bottega (2006) or Cai *et al.* (2002). In almost all structural problems, the resonance frequencies are relatively high, so the damping component related to the mass (the term involving α) is negligible. Therefore:

$$\xi = \frac{\beta\omega_i}{2} \quad (23)$$

For a cantilever beam, applying equation (7) we have, for the first natural frequency:

$$\beta = \frac{2\xi}{\omega_1} = 2\xi \sqrt{\frac{0,2424m_b L^3}{3EI}} \quad (24)$$

Materials and methods

Experimental set.

Experiments were carried out by fixing a specimen of the material vertically to the workbench. The free end of the specimen was then moved away from its equilibrium position, and allowed to vibrate freely. The displacement of the end of the specimen was measured for a time interval of 5 s.

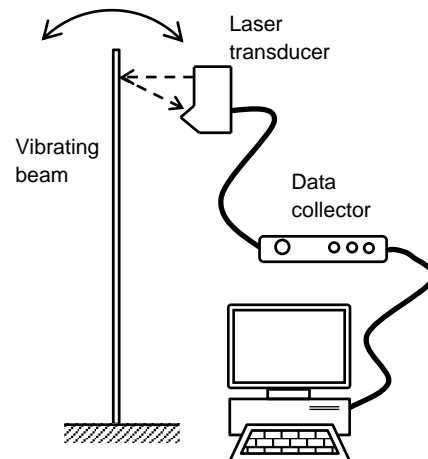


Fig. 2: Experimental set.

In order to measure the displacements, a laser transducer, which can record data with a frequency of up to 100 kHz, was used. The output of the transducer is an analog voltage signal. The distance to the object to be measured was 90 mm (SO, Fig.3). From this distance, a measurement range of 45 mm (MR) was permitted. For data collection a Spider8 recording system of HBM™ was used, which handles analog information

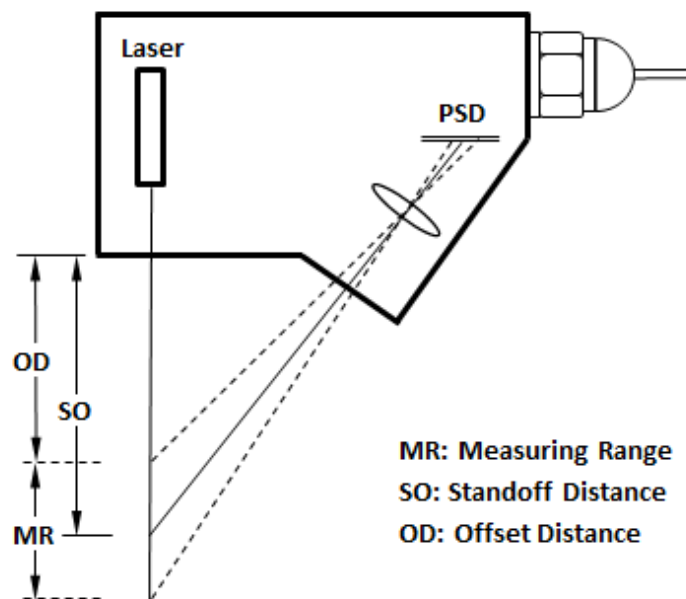


Fig. 3: Laser transducer.

Table 2: material of the studied specimens.

<i>Material</i>	<i>Usual applications</i>	<i>section of specimen [mm]</i>	<i>Density [kg/m³]</i>	<i>E [MPa]</i>
Steel 1020	general mechanics	10.5 x 2	7850	210000
DOCOL™	cold-rolled high strength steel for automotive industry	22 x 1	7760	200000
DOCOL 1200M™	high performance automotive applications steel: side impact beams, bumpers, seats and structural components	22 x 1	7730	197000
Aluminum 2030	tubes, bars, profiles, sheet	15 x 3	2760	57000
Polyethylene terephthalate (PET)	synthetic fibers, containers and packaging, engineering resins	12 x 2	1210	1580
Polypropylene (PPHM)	textiles, pipes, laboratory equipment, loudspeakers, automotive components, banknotes	11 x 2	1310	5140

processing, amplifies it and converts it into a digital signal. The digitized signal is treated with Catman™ software for post-processing.

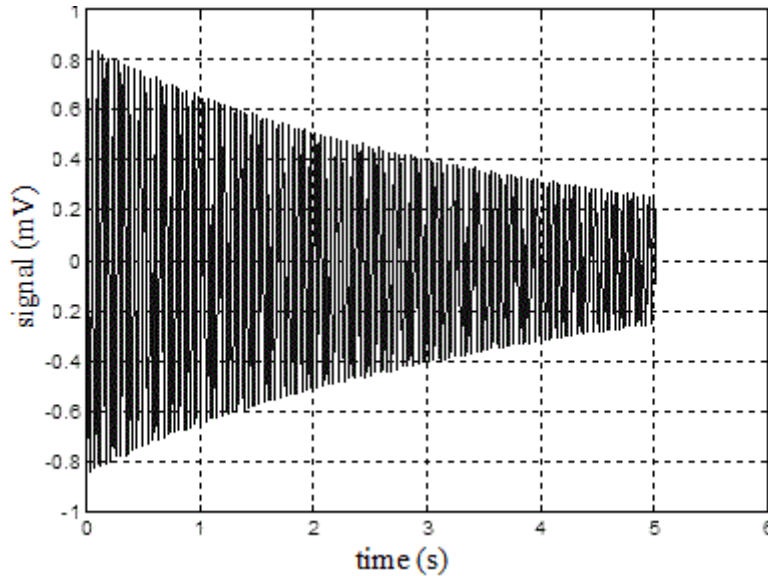


Fig 4: Experimental signal captured by the laser transducer, for the specimen of steel Docol1200M

Data obtained in this manner (Fig. 4) were introduced into the adjustment program coded in Matlab™, to obtain the natural frequency and damping ratio. Ten trials were performed for each material. Specimens of several materials were studied, according to Table 2.

A series of tests on the steel specimen were performed to test the consistency of the settings. Different lengths of cantilever beam were taken to cover a wide range of natural frequencies. Table 3 shows the results obtained for the natural vibration frequency, compared to the theoretical values expected according to equation (7).

Table 3: frequencies experimentally obtained for several lengths of cantilever of a steel specimen ($E = 210$ GPa, $density = 7850$ kg/m³).

L [mm]	f_1 [Hz] <i>experimental</i>	f_1 [Hz] <i>theoretical (7)</i>	<i>Difference</i> <i>in f_1</i>
130	85.4	98.9	-15.8%
150	68.0	74.3	-9.3%
170	53.0	57.9	-9.2%
190	41.5	46.3	-11.6%
210	34.7	37.9	-9.3%

The theoretical model does not consider damping, so part of the differences between the experimental frequency and the calculated frequency is the effect of damping. It must be stated that the differences seem to be too high, but the expression of the natural frequency is, from (7):

$$f_1 = \lambda \cdot h \cdot L^{-2} \cdot E^{1/2} \cdot \rho^{-1/2} \quad (25)$$

where λ is a generic constant. So, the relative error of the frequency is:

$$e_{f_1} = e_h + 2 \cdot e_L + \frac{1}{2} e_E + \frac{1}{2} e_\rho \quad (26)$$

where e is the relative error of each magnitude (Demidovich and Maron, 1987). Assuming 0.05 mm to be the measuring error for h (2.5% for $h=2\text{mm}$), 1 mm for L (0.8% for $L=130\text{mm}$), 5% for the values of density and 10% for E , the total relative error for the theoretical frequency is 10.8%. Such a variation, translated into the value of the damping ratio, can explain the difference found between the experimental frequency and the calculated frequency.

Determination of the optimal parameters for fitting experimental data.

The importance of the critical parameters to achieve good fits to the experimental data was studied. The effectiveness of adjusting the coefficients of equation (15) with experimental data is related to the correct choice of the initial values of optimization. Starting with coefficients close to their real value makes the convergence of the method quicker. On the other hand, a bad choice can mean that no convergence is reached and that the equation does not fit the experimental data. Before attempting to make a proper fit it is recommendable to briefly review the experimental data. For example, for the experimental data regarding the movement, the maximum value is recommended for an initial value x_0 .

In addition, in the case of a cantilever beam, it is possible to know its theoretical natural frequency ω_n (7), so that an evaluation of it would provide a good initial guess. The damping values can be taken depending on the material to be tested for a first approximation. In the literature, the approximate values of damping can be found, depending on the material, so these would be suitable for the values of ζ .

Besides a proper choice of initial coefficients, there are also two parameters which strongly influence the fit. The first parameter is the sampling interval Δt . The other parameter is the amount of periods taken for each setting n_T . If many periods are taken for analysis, the calculation time increases because of the dimensions of the vectors to be

analyzed (Fig. 5). This time increase seems to not be significant with the use of an Intel Core i5 CPU, 2.67 GHz but the effect was much larger with the original equipment used in the lab. On the other hand, if only a few oscillations are taken, they hardly represent a damped oscillatory motion and the fit will be incorrect too.

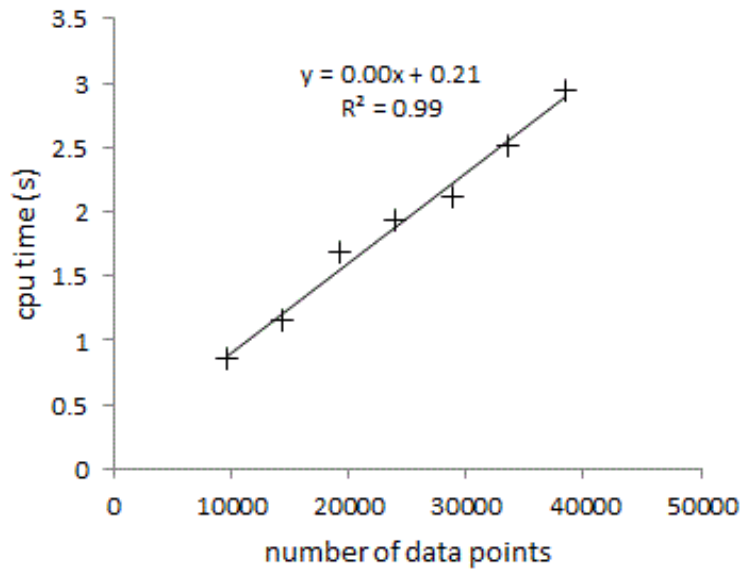


Fig. 5: Time of computation for increasing number of data points (with an Intel Core i5 CPU, 2.67 GHz).

To determine the correct values for these parameters, data were generated from expression (15) and the adjustment program was applied. This was done in order to establish the coefficients of the equation of the damped free movement of the signal using as initial values the same ones used to generate the data. Once the fit was achieved, the relative error of the values obtained for ω and ζ was measured. A calculation was made by taking periods 1, 2, 3 up to 10. The results are shown in Figure 4. If attention is focused on the target of the subroutine (measuring the damping factor), for two periods, the error is less than 0.01%. The other errors lie within an acceptable range (Fig. 6).

Sampling with an unsuitable frequency can lead to a great distortion in the information. Nyquist's theorem establishes that the sampling frequency must be at least twice the highest sampled frequency. Some literature recommends taking ten times the highest sampled frequency. For a generic case, the sampling period is:

$$T_s = \frac{1}{n \cdot f_{\max}} \quad (27)$$

where T_s is the sampling period, n the number of data for each period, and f_{max} the maximum frequency to be detected. For the virtual experiment, a full range of two periods was considered, as in the previous experiment this outcome was considered suitable.

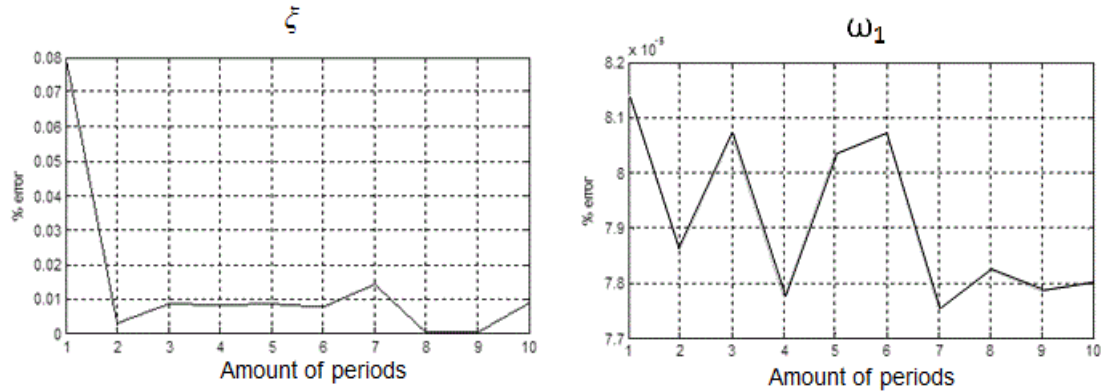


Fig. 6: Relative error (%) of the damping ratio and the natural frequency, depending on the amount of periods taken for the fitting.

The study was performed with two to twenty samples per period, taking as highest frequency $f_{max} = 1/\pi$ Hz, which is the frequency of the generated data. For a number of data per period higher than 2, the errors are below 1% for ζ and below $10^{-5}\%$ for ω_1 . For higher sampling frequencies, there is no significant improvement in the results.

Results and discussion

Damping ratio measurement.

Table 4 shows the results of the resonance frequency and damping ratio of the specimens of the studied materials. The resonance frequency is comparable to that calculated theoretically using equation (7).

There are several ways of taking damping into account in AnsysTM calculations. The most general way is by using *Alpha & Beta Damping* or *Rayleigh Damping*. For high frequencies, the α term (22) can be disregarded and the constant β can be calculated using equation (24) in the case of a cantilever beam.

The value of β for the Aluminum 2030 specimen was calculated by equation (24). This value has been used to simulate the vibration of the specimen in AnsysTM. For the calculations, the time step was equivalent to the sampling frequency used in the experiments, in order to have the same number of data. Finally, the signal (displacement of the free end) obtained from the simulation was introduced into the fitting program in

order to obtain ω_1 and ζ . The value of the damping ratio obtained experimentally was 0.277 %, whilst the one obtained from the simulation signal was 0.283 %. The relative difference is 2 %.

Table 4: natural frequencies and damping ratio for several materials ($L = 170$ mm). Experimental and theoretical values from the equation (7).

Material	ζ [%]	f_1 experimental [Hz]	f_1 theoretical [Hz]	difference in f_1
steel	0.15	53.1	57.9	-8%
DOCOL™	0.19	25.4	28.4	-11%
DOCOL 1200M™	0.19	25.4	28.2	-10%
Al 2030	0.27	74.5	76.2	-2%
PET	0.56	13.3	12.8	4%
PP HM	1.36	24.2	22.2	9%

In addition to what has already been stated about the range of error in the data used for the calculation, there is a certain correlation between the damping ratio and the difference of frequency values as can be seen in figure 7. The higher the value of damping, the greater the difference between the theoretical and experimental values of frequency. This makes sense since the theoretical value is obtained from a model without damping.

The same study was carried out for the vibration of a sample with a mass attached to the free end under bending loads. The goal was to verify that the damping ratio obtained from the former tests could be used in a numerical simulation of a case with a different load. In addition, it was compared to the theoretical value (12).

A vibration test was performed with a specimen of Al2030, with a mass of 60 grams attached to the free end. This experiment was simulated by using 50 bi-dimensional elements BEAM3 and MASS21 of Ansys™. The frequency of the first mode of vibration obtained from the modal analysis was 21.02 Hz, while the

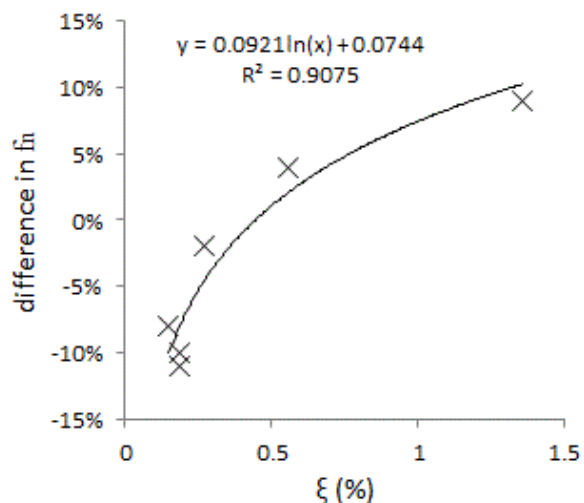


Fig. 7: Correlation between damping ratio and difference on frequency (theoretical and experimental).

result from solving the theoretical equation (12) was 21.01 Hz and from experimental testing 23.00 Hz. The difference is 8.7%

Methodology validation: Measurement of the damping ratio of a structure.

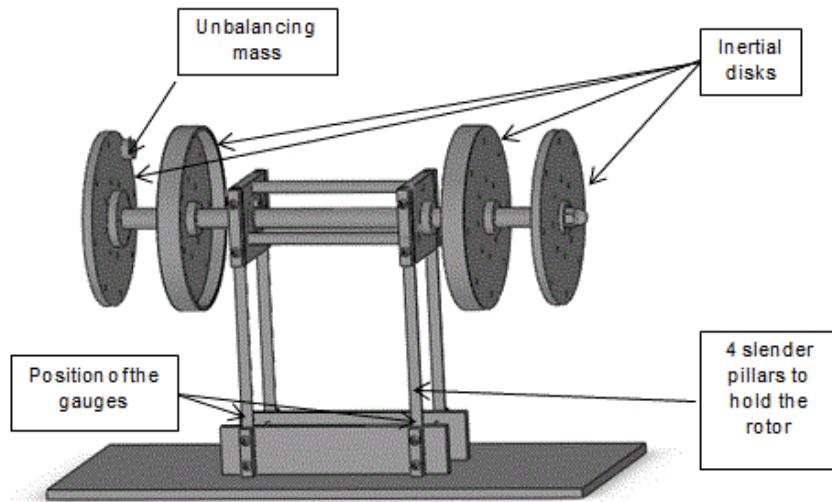


Fig. 8: An inertial rotor which can be unbalanced, supported by 4 beams. Two gauges measure the deformation of the beams.

In order to validate the applicability of the methodology, a complex spatial structure holding an unbalanced rotor was simulated and tested as shown in Fig. 8. Damping ratios obtained in previous sections were used to feed simulation data. Experimental results obtained with extensometers validated simulation results.

An unbalanced rotor supported on a four vertical steel bar structure was used as a test structure (Fig. 8). Two of the beams were equipped with extensometric gauges. The rotor starts with an initial velocity higher than the natural frequency of the system and the unbalanced rotor produces harmonic excitation bending support beams. The large mass of rotor plus a small unbalanced mass, is placed as a cantilever tip mass. As the rotor slows down, the exciting force decreases going first through its torsional resonance and then, with a slower rotating speed, through its bending resonance (Fig. 9). The strain at the gauges was captured and recorded by the computer.

From the measured strain gauge and the translation of this value into displacement, the resonance frequency of the structure and its damping ratio may be calculated. Performing a Discrete Fourier Transform (by FFT algorithm) the values of the two resonance

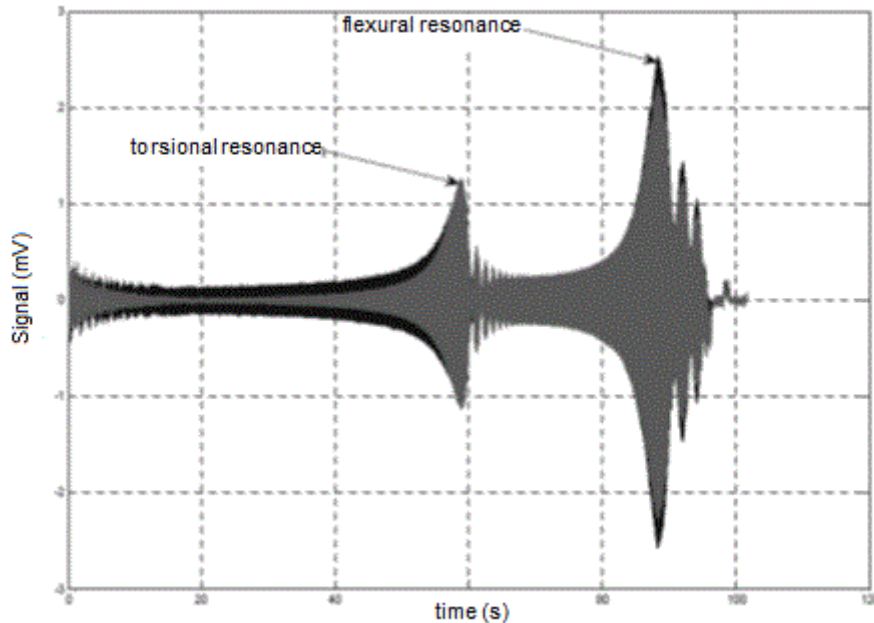


Figure 9: Signal of displacement at the base of the two (gray / black) mounting plates, with the points of resonance.

frequencies (Fig. 10) were obtained. Those frequencies were 9.30 Hz (torsion) and 6.83 Hz (bending). The damping ratio was calculated from the dynamic amplification which was around 50 and therefore leading to a damping ratio of around 1% at 6.83 Hz, much larger than the 0.15% measured at 53.1 Hz for the same steel of the beams. This issue arises from the fact that the speed dropped too fast and there were not enough cycles in resonance frequency to amplify the signal to its maximum value.

The balancing machine was simulated with Ansys TM using a simplified model of four rectangular section beams, each one divided into 50 elements (BEAM188). The four beams were fixed by one end. At the free end they were attached to a mass point element (MASS21) having the properties (mass and moment of inertia) of the whole top of the machine (mass: 5.674 kg; $I_{xx} = 16749 \text{ kg}\cdot\text{mm}^4$, $I_{yy} = 166418 \text{ kg}\cdot\text{mm}^4$ and $I_{zz} = 166758 \text{ kg}\cdot\text{mm}^4$, where the z axis is vertical and downward; the x axis is horizontal and coaxial with the rotor; and the y axis is horizontal and transverse to the axis of rotation of the rotor).

Once a modal analysis of this model was performed, the first two natural frequencies corresponding to the resonance frequencies of torsion and bending were obtained. These values, compared with those obtained experimentally, are shown in Table 5.

Table 5: resonance frequencies of the structure [Hz].			
	<i>Experimental</i>	<i>Modal analysis</i>	<i>Virtual (28) (29)</i>
<i>Bending</i>	6.83	6.97	7.80
<i>Torsion</i>	9.30	10.35	11.76

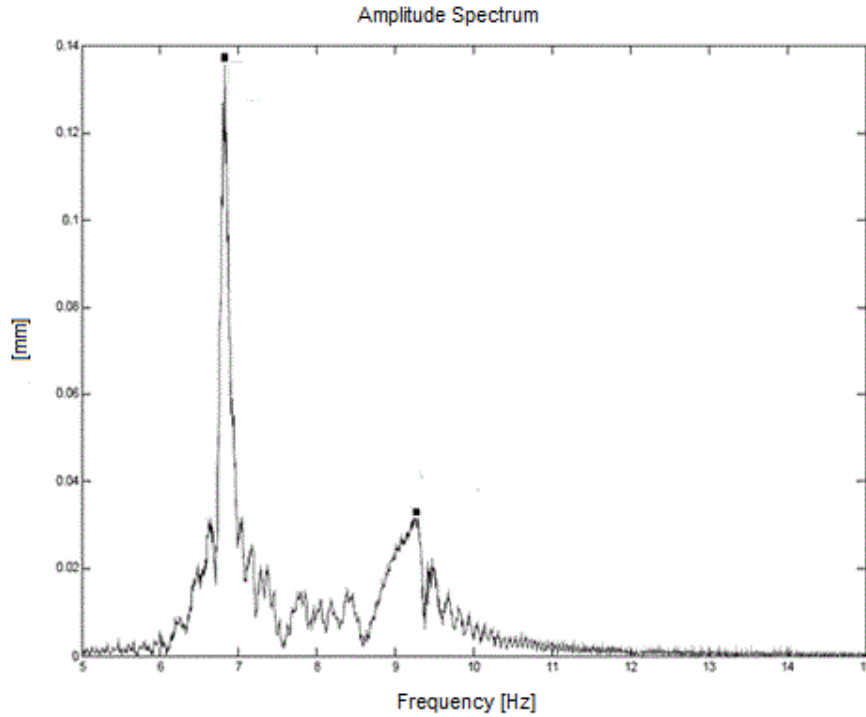


Fig. 10: Frequency spectrum of the mV signal of strain gauge in figure 9, obtained by DFT and translated into mm of displacement.

Furthermore, through virtual experiments, the bending and torsional stiffness were determined. Mass was measured and compared to the computer model of the system. Inertia was taken directly from the computer model. From these values of stiffness, mass and inertia, the resonance frequencies were calculated using the formulas for the linearized model:

$$\omega_{1,flex} = \sqrt{k_{flex}/m} \quad (28)$$

$$\omega_{1,tor} = \sqrt{k_{tor}/I_z} \quad (29)$$

Results are shown in Table 5.

Conclusions

A new method to calculate damping properties of rigid materials to be used in FEM calculations is presented. The method is simple and no expensive equipment is needed. No report of a similar method has been found in consulted literature.

The results obtained in simulation have shown a good match with physical models tested. By applying it, errors under 0.1 % were obtained. The fitting algorithm converges very quickly, and also provides a value for the sum of the errors, which informs about the accuracy of the adjustment.

Recommendations to select initial parameters are presented. Critical parameters to achieve good mathematical fits of the experimental data are identified, described and demonstrated.

The correlation between theoretical data reported in literature, simulation and experimental results is presented and discussed. Several materials were tested with varying mass and geometrical properties of specimens in order to assure confidence in the method if used in industrial applications.

The application to a complex hyperstatic three-dimensional structure proves the validity of this method and its applicability to real world situations.

References

- ASTM E756-05. (2010) Standard test method for measuring vibration-damping properties of materials.
- Bottega WJ (2006) *Engineering Vibrations*. Boca Raton (FL): CRC – Taylor & Francis.
- Brodthorn M and Lakes RS (1995) Composite materials which exhibit high stiffness and high viscoelastic damping, *Journal of Composite Materials* 29: 1823-1833.
- Cai C, Zheng H, Khan MS and Hung KC (2002) Modeling of Material Damping Properties in ANSYS, *2002 International ANSYS Conference Proceedings*, <http://www.ansys.com/staticassets/ANSYS/staticassets/resourcelibrary/confpaper/2002-Int-ANSYS-Conf-197.PDF>; (accessed 26/01/2014).

- Cai Ch and Sun Q (2010) Measurement and evaluation of damping properties of damping material. In: *IMEKO 2010 TC3, TC5 and TC22 Conferences*, Pattaya (Thailand).
- Chowdhury I and Dasgupta SP (2003) Computation of Rayleigh Damping Coefficients for Large Systems, *The Electronic Journal of Geotechnical Engineering* 8, www.ejge.com/2003/Ppr0318/Ppr0318.pdf; (accessed on 2013/04/29).
- Crespo JE, Juliá E, Parres F, Segura J, Gadea JM and Nadal AV (2010) Investigation of damping properties using products coming from ELT (end-of-life-tires), *Annals of the Oradea University. Fasc. Management and Technological Engineering*, 9 (19): 21-24.
- Demidovich BP and Maron IA (1987) *Computational mathematics*. Moscow: Mir Publishers.
- Erdoğan G and Bayraktar F (2003) Measurement of dynamic properties of materials. In: *The 32nd International Congress and Exposition on Noise Control Engineering*, Seogwipo, (Korea).
- Foss GC (2007) Viscoelastic damper performance testing. In: *SEM – Proceedings of IMAC XXV* (2007). Available at www.sem.org/Proceedings/, (accessed on 2013/01/22).
- Gatti PL and Ferrari V (1999) *Applied structural and mechanical vibrations*. London: Taylor & Francis.
- Hammami L, Zghal B, Fakhfakh T and Haddar M (2005) Characterization modal damping sandwich plates, *Journal of Vibration and Acoustics*, 127: 431 -440.
- Ilg J, Rupitsch SJ, Sutor A and Reinhard Lerch R (2012) Determination of dynamic material properties of silicone rubber using one-point measurements and finite element simulations, *IEEE Transactions on Instrumentation and Measurement*, 61(11): 3031-3038.
- Jáuregui JC, Urbiola L, Díaz C and Aboites F (2005) Modelado multidimensional de sistemas viscoelásticos, *Ingeniería Mecánica: Tecnología y Desarrollo* 2(1): 6-12.
- Malogi D, Gupta A and Kathawate GR (2009) Center impedance method for damping measurement, *Advances in Acoustics and Vibration*. DOI:10.1155/2009/319538.
- Martinez-Agirre M and Elejabarrieta MJ (2010) Characterisation and modeling of viscoelastically damped sandwich structures, *International Journal of Mechanical Sciences* 52(9): 1225–1233.

Newland DE (1989) *Mechanical Vibration Analysis and Computation*, Longman, New York.

Orban F (2011) Damping of materials and members in structures, 5th International Workshop on Multi-Rate Processes and Hysteresis (MURPHYS 2010), *Journal of Physics: Conference Series* 268. DOI:10.1088/1742-6596/268/1/012022.

Rao SS (1986) *Mechanical Vibrations*, Addison-Wesley, Reading (MA).

Wei CY and Kukureka SN (2000) Evaluation of damping and elastic properties of composites and composite structures by the resonance technique, *Journal of Materials Science* 35(15): 3785-3792.

Wojtowicki JL, Jaouen L and Panneton R (2004) New approach for the measurement of damping properties of materials using the Oberst beam, *Review of Scientific Instruments*, 75(8): 2569-2574.

Xu Y and Nashif A (1996) Measurement, analysis and modeling of the dynamic properties of materials, *Sound & Vibration* 30(7): 20-23.